Supplementary Information

PDZ binding of TARP γ-8 controls synaptic transmission, but not synaptic plasticity

Akio Sumioka[1, 2, 5], Travis Brown[3, 5], Akihiko Kato[4], David S. Bredt[4], Julie A. Kauer[3*], and Susumu Tomita[1, 2*]

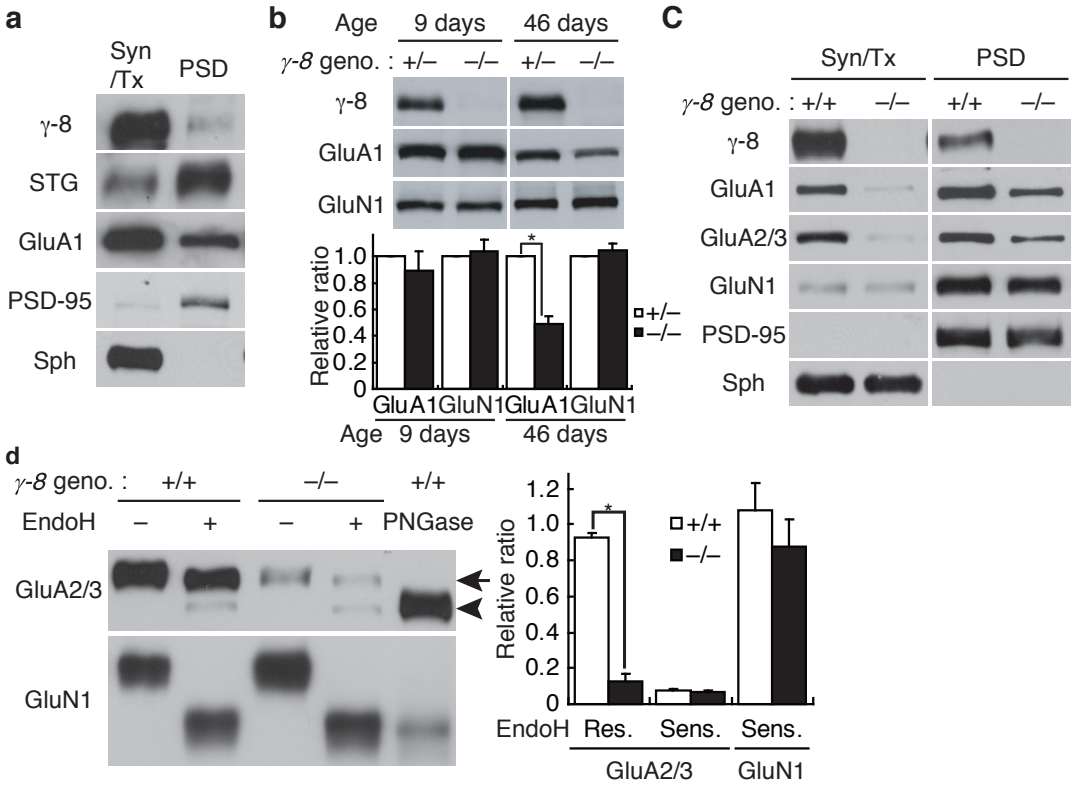

Supplementary Figure 1 TARPγ-8 stabilizes AMPARs in hippocampus. (**a**) Differential distribution of γ-8 and γ-2/stargazin in mouse hippocampi. Mouse hippocampi were fractionated as Triton-solubilized synaptosome (Syn/Tx) and PSD fraction, and the same volume of samples were loaded in each lane. (**b**) GluA1 protein expression is reduced only in hippocampi from adult (P46), but not juvenile (P9) γ-8 knockout (γ-$8^{-/-}$) mice. (**c**) AMPAR expression (GluA1 and GluA2/3) was reduced much more in the Triton-solubilized synaptosome (Syn/Tx) fraction than in the PSD fraction. (**d**) Mouse hippocampal lysates were treated with EndoH glycosidase. EndoH-resistant GluA2/3 levels (Arrow; Res.) were reduced in γ-$8^{-/-}$ mice without changes in the amount of EndoH-sensitive AMPARs (Arrowhead; Sens.). PNGase treatment provided the molecular weight of GluA2/3 without N-glycosylation. GluN1 glycosylation is known to be EndoH-sensitive[1]. All data are given as mean ± s.e.m (n=4).

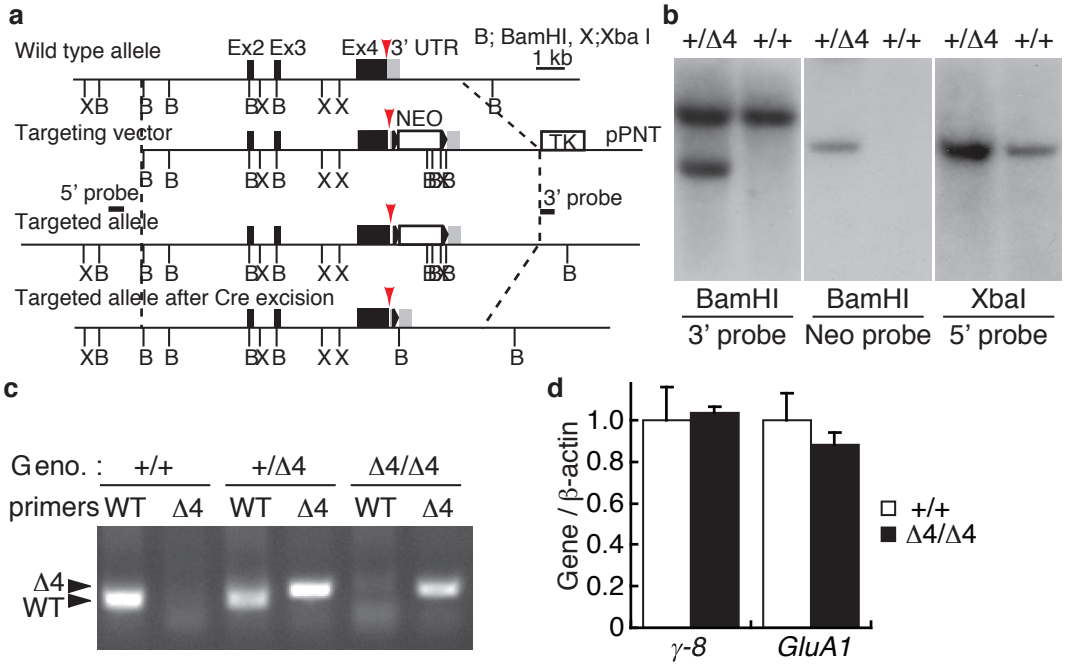

Supplementary Figure 2 Generation of the γ-8Δ4 knock-in mice ($\gamma\text{-}8^{\Delta4/\Delta4}$). (**a**) Schematic representation of genomic locus for *γ-8* gene, targeting vector, targeted allele and targeted allele after excision of LoxP cassette by Cre recombinase. The exon 4 of γ-8 was replaced by homologous recombination with mutated exon 4 in which the C-terminal 4 amino acids were deleted (red arrow-head). Lox P sites (triangle) were flanked with a neomycin resistant gene (LoxP cassette). (**b**) Confirmation of homologous recombination by southern blotting. A probe for 3' genomic region (3' probe) yielded two bands in $\gamma\text{-}8^{+/\Delta4}$ clone, and a single band in WT ($\gamma\text{-}8^{+/+}$). A probe for the neomycin gene yielded a single band in γ-8Δ4 clone, and no signal in $\gamma\text{-}8^{+/+}$. A probe for 5' genomic region yielded a single band in both $\gamma\text{-}8^{+/\Delta4}$ clone and $\gamma\text{-}8^{+/+}$. (**c**) Genotypes of targeted allele confirmed by PCR reaction. WT, wild-type; $\gamma\text{-}8^{+/\Delta4}$, heterozygous; $\gamma\text{-}8^{\Delta4/\Delta4}$, homozygous knock-in. (**d**) mRNA expression levels in hippocampi of $\gamma\text{-}8^{+/+}$ (WT) mice and $\gamma\text{-}8^{\Delta4/\Delta4}$ mice are determined by quantitative PCR with SYBR green. Relative signals of both *γ-8* and *GluA1* (normalized to β-actin) in $\gamma\text{-}8^{\Delta4/\Delta4}$ mice were similar with those in WT mice. All data are given as mean ± s.e.m.

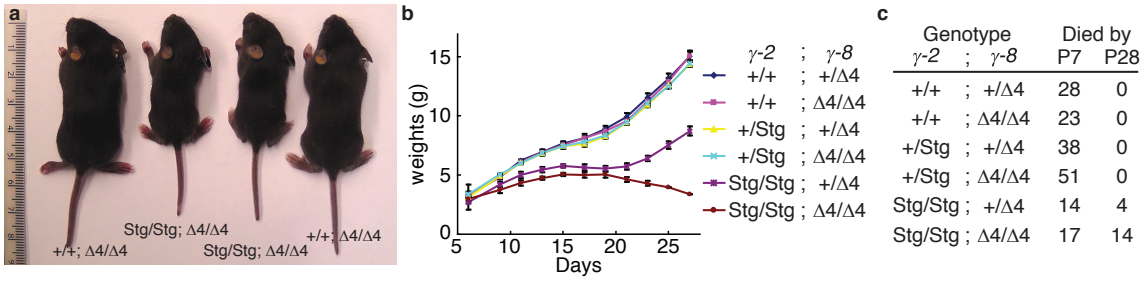

Genotype γ-2 ; γ-8	Died by P7	P28
+/+ ; +/Δ4	28	0
+/+ ; Δ4/Δ4	23	0
+/Stg ; +/Δ4	38	0
+/Stg ; Δ4/Δ4	51	0
Stg/Stg ; +/Δ4	14	4
Stg/Stg ; Δ4/Δ4	17	14

Supplementary Figure 3 γ-8Δ4/stargazer double mutant mice have a severe defect in development. (**a**) Photographs of mice with the indicated genotypes at P24. (**b, c**) Mouse survival and growth curves of indicated genotypes resulting from breeding a male ($\gamma\text{-}2^{+/stg};\gamma\text{-}8^{\Delta4/\Delta4}$) and female ($\gamma\text{-}2^{+/stg};\gamma\text{-}8^{+/\Delta4}$). Growth defects were observed, and 14 of 17 double mutant mice were dead by P28. Using Kaplan-Meier Survival analysis and the logrank test, we observed a significant reduction in survival rate of both double homozygous mutant mice ($\gamma\text{-}2^{stg/stg};\gamma\text{-}8^{\Delta4/\Delta4}$) and γ-2 homozygous/γ-8Δ4 knock-in heterozygous ($\gamma\text{-}2^{stg/stg};\gamma\text{-}8^{+/\Delta4}$) from the other genotypes shown.

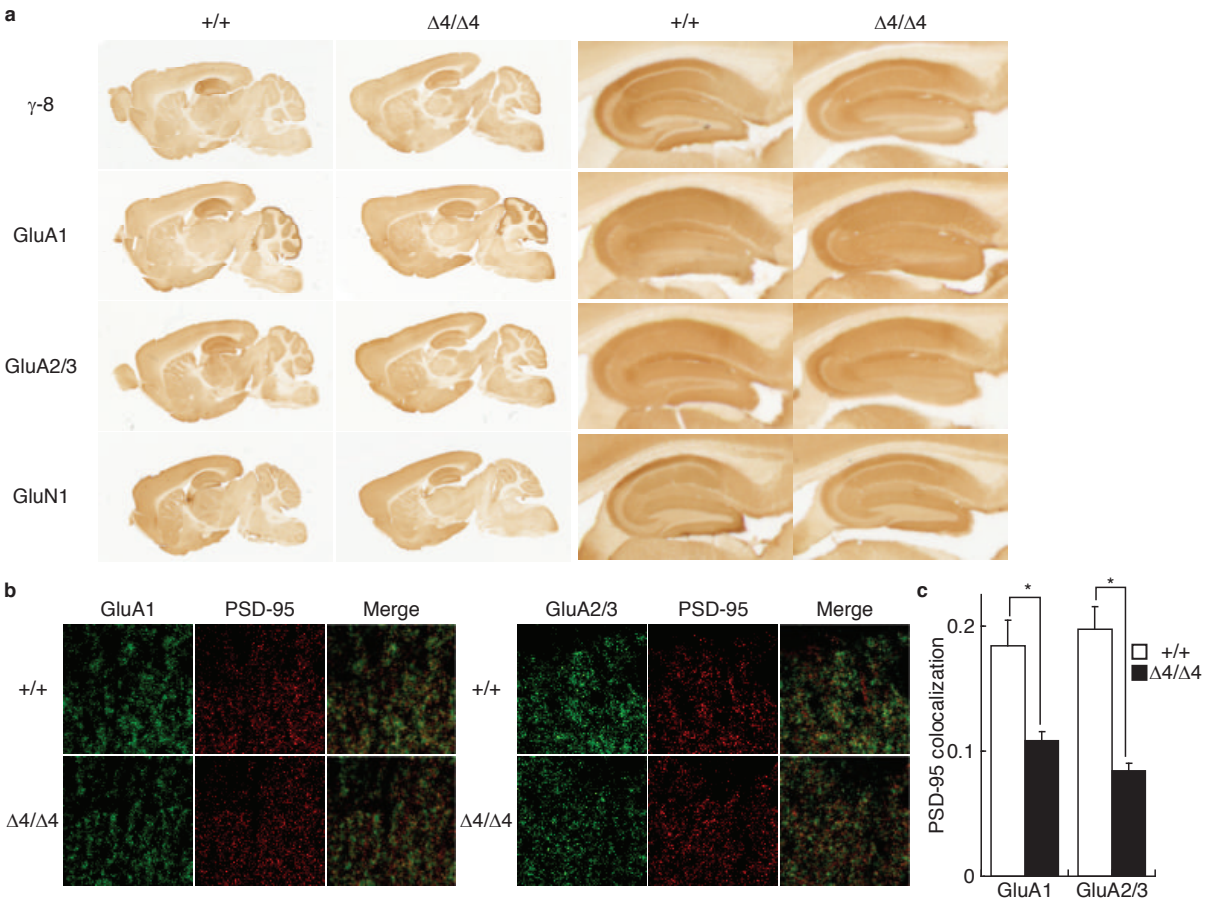

Supplementary Figure 4. Co-localization of AMPAR with PSD-95 is reduced in TARP γ-8Δ4 knock-ins without an obvious difference in AMPAR global distribution. (**a–c**) Immunohistochemical staining of sagittal brain sections from $\gamma\text{-}8^{+/+}$ and $\gamma\text{-}8^{\Delta4/\Delta4}$ mice. (**a**) No obvious difference in distribution of γ-8, AMPA receptor subunit (GluA1 and GluA2/3) or NMDA receptor subunit (GluN1) was observed in hippocampus from $\gamma\text{-}8^{+/+}$ and $\gamma\text{-}8^{\Delta4/\Delta4}$ mice. (**b, c**) Double immunostaining of AMPA receptor and PSD-95 showed reduction in co-localization of AMPAR with PSD-95 in hippocampus from $\gamma\text{-}8^{\Delta4/\Delta4}$ mice. All data are given as mean ± s.e.m (n=10).

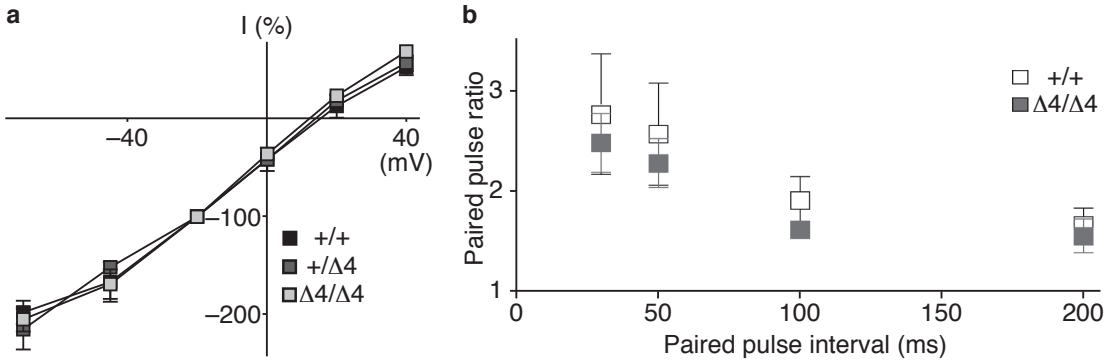

Supplementary Figure 5 No difference in the I-V relationship (**a**) or paired-pulse ratio **(b).** Current-voltage plots of evoked AMPAR EPSCs were similar in cells from γ-$\delta^{+/+}$ (black; n=6), γ-$\delta^{\Delta4/\Delta4}$ (light grey; n=10) and γ-$\delta^{+/\Delta4}$ mice (grey; n=11). Data were normalized to values at -20 mV. **(b)** Paired-pulse ratios do not differ between cells from γ-$\delta^{+/+}$ (open squares; n=3) and γ-$\delta^{\Delta4/\Delta4}$ mice (grey squares; n=5). All data are given as mean ± s.e.m.

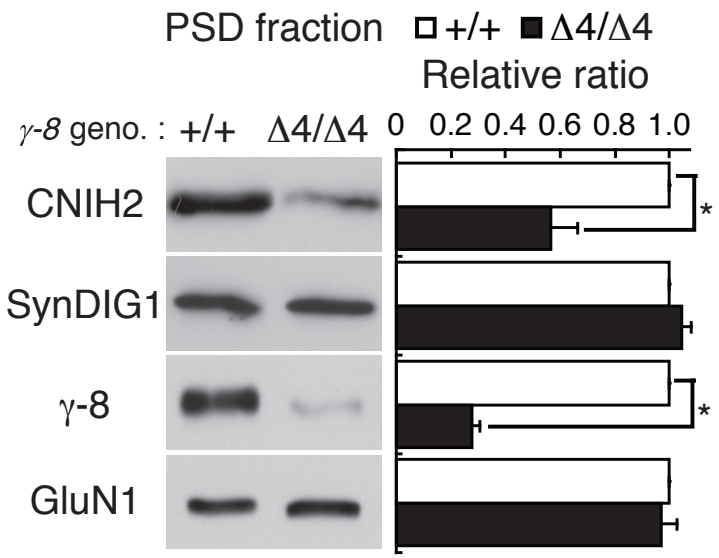

Supplementary Figure 6 TARPγ-8/AMPAR complex stabilizes CNIH2 in the hippocampal PSD fraction. CNIH2 expression in the PSD fraction was significantly reduced in $\gamma\text{-}8^{\Delta4/\Delta4}$ mice, whereas GluN1 and SynDIG1 were not. All data are given as mean ± s.e.m.; * $P < 0.05$.

Supplementary Figure 7. Full and uncropped blot pictures in the main figures

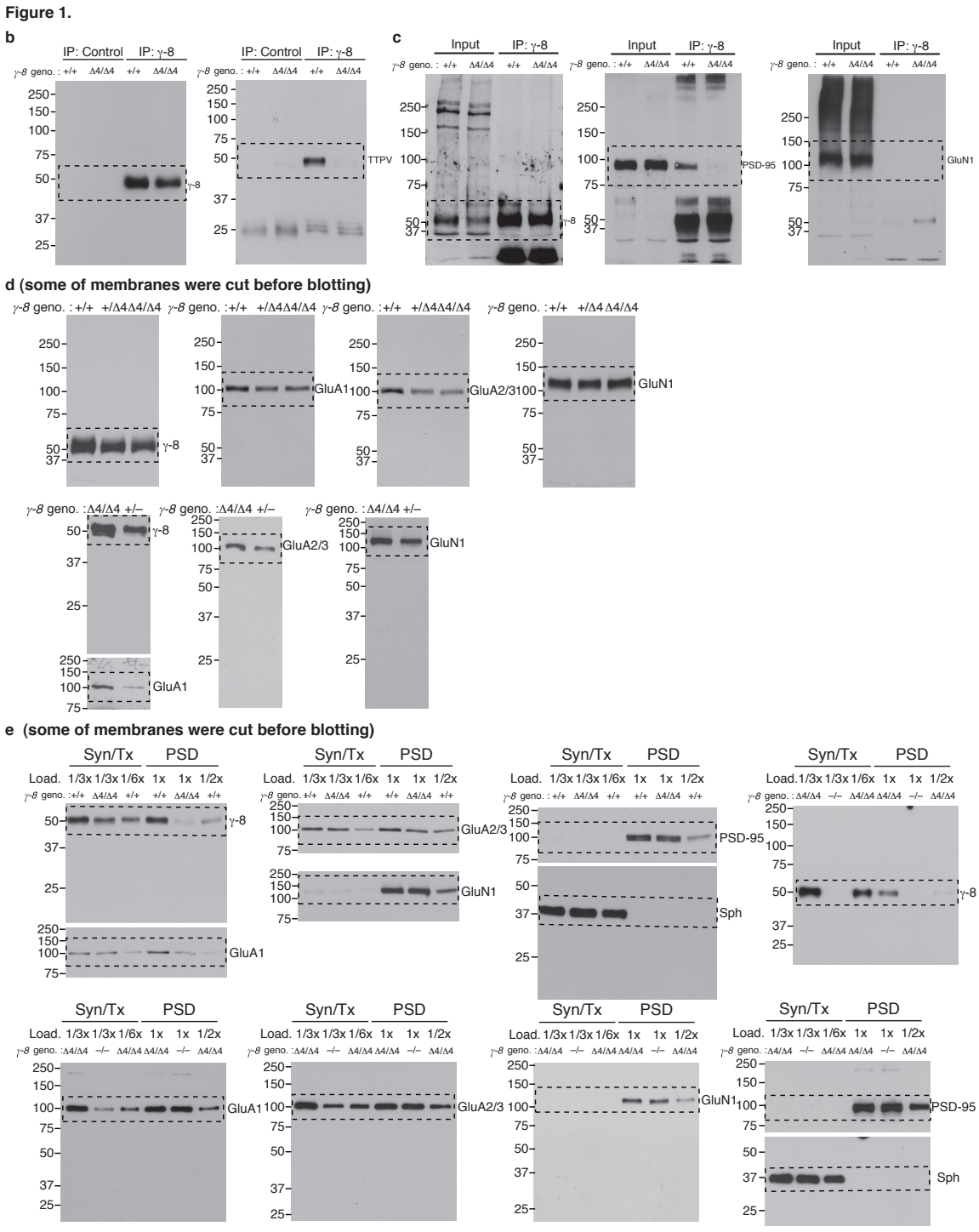

Methods

Antibodies

Mouse monoclonal antibodies were used against PSD-95 (ABR), GluN1 (Pharmingen) and SynDIG1 (NeuroMab). Rabbit polyclonal antibodies were used against the following proteins; γ-8 and TTPV[2]; GluA1, GluA2/3 (Millipore) and synaptophysin (Sigma). Guinea pig polyclonal antibody was used against CNIH2[3].

Generation of γ-8Δ4 knockin

The targeting vector is designed to replace exon 4 with a mutated exon, which encodes the C-terminal cytoplasmic domain lacking the C-terminal 4 amino acids together with a lox P-flanking neomycin resistant gene. The targeting vector was linearized, and electroporated into mouse embryonic stem (ES) cells. After selection with neomycin and Hsv-Tk, ES colonies were picked up and expanded. Proper homologous recombination was confirmed by Southern blotting. The targeted ES cells were injected into blastocysts and implanted into surrogate mothers. Chimeric mice were identified by genotype PCR, and mated with actin-Cre mice to remove the neomycin resistance gene. All mice were maintained at the Yale animal resource center under the guidelines of the institutional animal care and use committee.

Protein analysis of the mice brains

For analysis of total protein amounts, hippocampi were homogenized and solubilized in 1 % SDS/TE. PSD fractionation from hippocampi and co-immunoprecipitation were performed as previously described[2,4]. Briefly, the synaptosomal fraction was isolated from the hippocampal P2 fraction by sucrose density gradient centrifugation. The PSD fraction was then isolated as Trion X-100 insoluble materials of the synaptosomal fraction.

Immunostaining

Staining was done as previously described[2]. The sections were processed to Vectastain ABC kit (Vector laboratories) protocol using DAB substrate, or stained with fluorescent secondary antibody and analyzed with confocal microscopy (Zeiss, LSM510).

Synaptic electrophysiology

Coronal slices through the hippocampus were prepared from wild-type, heterozygote and homozygote TARP γ-8Δ4 knockin mice and from TARP γ-8 knockout mice, P28-P56, as detailed previously[5]. All animal protocols were approved by the Brown University Institutional Animal Care and Use Committee. Only one slice per mouse was used for each experiment so that reported n values represent the number of animals. Recording conditions and solutions for whole-cell and field potential recordings from CA1 pyramidal cells were as described[5]. For AMPA/NMDA ratios, neurons were held at +40 mV and 50 μM d-APV was added. Peak AMPAR EPSC amplitudes were measured at 10-15 minutes in d-APV, and this EPSC was subtracted from 5 minute averages of basal

EPSCs to obtain the peak NMDAR EPSC. I-V curves were obtained in 100 μM picrotoxin and 50 μM d-APV; all values were normalized to the EPSC amplitude at -20 mV. To induce LTP in whole-cell mode, depolarization to 0 mV was paired with 1 Hz afferent stimulation for one minute within 12 minutes of break-in to the whole-cell configuration.

Statistical analysis

All data are given as mean ± s.e.m. Statistical significance between means was calculated using unpaired Student's t test. In all figures, error bars indicate ± s.e.m..

References

1. Kato, A., Rouach, N., Nicoll, R.A. & Bredt, D.S. Activity-dependent NMDA receptor degradation mediated by retrotranslocation and ubiquitination. *Proc Natl Acad Sci U S A* **102**, 5600-5605 (2005).
2. Tomita, S.*, et al.* Functional studies and distribution define a family of transmembrane AMPA receptor regulatory proteins. *J Cell Biol* **161**, 805-816 (2003).
3. Kato, A.S.*, et al.* Hippocampal AMPA receptor gating controlled by both TARP and cornichon proteins. *Neuron* ***68***, 1082-1096 (2010).
4. Jo, K., Derin, R., Li, M. & Bredt, D.S. Characterization of MALS/Velis-1, -2, and -3: a family of mammalian LIN-7 homologs enriched at brain synapses in association with the postsynaptic density-95/NMDA receptor postsynaptic complex. *J Neurosci* **19**, 4189-4199 (1999).
5. Gibson, H.E., Edwards, J.G., Page, R.S., Van Hook, M.J. & Kauer, J.A. TRPV1 channels mediate long-term depression at synapses on hippocampal interneurons. *Neuron* **57**, 746-759 (2008).